Evidence for γ vibrations and shape evolutions through the transitional ^{184,186,188,190}Hg nuclei

J. P. Delaroche and M. Girod
Commissariat à l'Energie Atomique, Service de Physique et Techniques Nucléaires, Boite Postale 12, 91680 Bruyères-le-Châtel, France

G. Bastin, I. Deloncle, F. Hannachi, J. Libert,* and M. G. Porquet
Institut National de Physique Nucléaire et de Physique des Particules, Centre National de la Recherche Scientifique, Centre de Spectrométrie Nucléaire et de Spectrométrie de Masse, 91405 Orsay, France

C. Bourgeois, D. Hojman,† P. Kilcher, A. Korichi, F. Le Blanc,
N. Perrin, B. Roussière, J. Sauvage, and H. Sergolle
Institut National de Physique Nucléaire et de Physique des Particules, Centre National de la Recherche Scientifique, Institut de Physique Nucléaire, 91406 Orsay, France

(Received 25 May 1993; revised manuscript received 27 May 1994)

Constrained Hartree-Fock-Bogoliubov calculations based on Gogny's force have been performed to determine the potential energy surfaces, collective masses, and moments of inertia used to build a five-dimension collective Hamiltonian treating quadrupole motion in the ^{184,186,188,190}Hg isotopes. Many collective states have been predicted at low excitation energy, some of them forming γ-vibrational bands. To expand experimental information on γ bands, high statistics measurements on the β^+ and electron capture decay of ^{190}Tl^{g,m} and ^{186}Tl^{g,m} have been performed at the ISOCELE facility. For the first time, γ bands have been identified in ^{190}Hg and ^{186}Hg. These new results together with previous experimental information available on the ground state and $K=0$ excited bands in ^{184,186,188,190}Hg form a database which has been analyzed and discussed in the present theoretical framework. It is argued that the first $K=0$ excited band in ^{190}Hg is a β-vibrational band, and that ^{186}Hg is a nucleus in which shape coexistence occurs not only for the $K=0$ bands but also for the γ bands.

PACS number(s): 21.60.Jz, 21.10.Re, 21.10.Ky, 23.20.Lv

I. INTRODUCTION

The neutron-deficient Hg isotopes have revealed over the years a rich variety of behavior. A spectacular odd-even staggering in $\delta\langle r^2\rangle$ (i.e., the change in the mean square charge radius) was observed for $A \leq 186$ from isotope shift measurements [1–3]. The abrupt change seen in $\delta\langle r^2\rangle$ between A=186 and 185 was interpreted as a shape transition [4–6] while the isomeric shift in ^{185}Hg was explained in terms of shape coexistence phenomena [7], a picture already suggested from nuclear spectroscopic measurements [8–11]. Furthermore, many excited rotational bands observed for the neutron-deficient Hg isotopes from in-beam experiments were explained as two quasiparticle neutron and proton excitations [12–14].

In the even-even Hg isotopes with $180 \leq A \leq 188$, shape coexistence phenomena are seen at low spin and excitation energy as two interacting collective bands with rather different moments of inertia [9–18]. It is a widespread belief that these bands are located at two distinct minima of comparable depth in the potential energy surface (PES). With this picture, the ground-state (g.s.) band is associated with a weakly oblate or near spherical shape, and the first excited band with a large prolate deformation. All the existing calculations, based either on the Strutinsky renormalization plus BCS pairing approach treating [19] or ignoring [20–22] triaxiality, or on the Hartree-Fock plus BCS [23] and Hartree-Fock-Bogoliubov (HFB) [24] theories, produce PES's showing two minima: one at quadrupole deformation $\beta \sim -0.12$ (oblate shape) and the other at $\beta \sim 0.25$ (prolate shape).

If coexistence between these two different nuclear shapes is well established in the light even-even Hg isotopes with $A \leq 188$, the situation is rather unsettled for heavier isotopes. For instance, algebraic and shell model studies [25,26] together with Nilsson-Strutinsky calculations [27] suggest the persistence of shape coexistence in ^{190}Hg; the Woods-Saxon Strutinsky calculations of Bengtsson *et al.* do not [19]. On the other hand, recent radioactive decay measurements [28] for ^{190}Tl have been interpreted as supporting shape coexistence in ^{190}Hg which parallels that established in ^{180,182,184,186,188}Hg.

In this work we first examine the following dilemma: Is shape coexistence ending abruptly for $A > 188$, or does it persist in heavier Hg isotopes, for instance, in ^{190}Hg? Here microscopic structure calculations have

*Present address: Centre d'Etudes Nucléaires de Bordeaux Gradignan, Le Haut Vigneau, 33170 Gradignan, France.
†Permanent address: Departamento de Física, Comisión Nacional de Energía Atómica, 1429 Buenos Aires, Argentina.

been performed for ^{184,186,188,190}Hg in a systematic effort to clarify this issue. It will be shown from the predicted positive-parity ($\pi = +$) levels and calculated reduced transition probabilities $B(E2; I_i \rightarrow I_f)$ for electric quadrupole transitions that the shape coexistence picture does not need to be invoked to explain the experimental results obtained by Kortelahti *et al.* [28] for ^{190}Hg. The second and main scope of our work is the identification of γ bands which are predicted at low excitation energy in neutron-deficient Hg isotopes. They have been searched for in ^{186,190}Hg from high-statistics measurements on the β^+ and electron capture (EC) decay of ^{190}Tl^{g,m} and ^{186}Tl^{g,m} produced at the Orsay on-line isotope separator ISOCELE.

This paper is organized as follows. In Sec. II we present the theoretical framework in which the collective levels and their γ-decay properties are calculated. The high-statistics γ-γ coincidence and γ-γ angular-correlation measurements from which spin values are deduced for $\pi = +$ states in ^{186,190}Hg are described in Sec. III. A comparison between our model predictions and experimental results is presented in Sec. IV. This is extended in Sec. V to the ^{184,188}Hg isotopes in order to trace the shape evolution taking place through the neutron-deficient Hg isotopes. Preliminary reports on this work can be found in Ref. [29].

II. THEORY

The theoretical framework within which are described the $\pi = +$ collective states at low spin and excitation energy is the generator coordinate method [30].

In the first step, potential energy surfaces (PES's) are built from constrained Hartree-Fock-Bogoliubov (HFB) calculations, i.e., from a minimization of the energy functional [31]

$$\delta\langle\Phi_q|\hat{H} - \lambda_0\hat{Q}_{20} - \lambda_2\hat{Q}_{22} - \lambda_Z\hat{Z} - \lambda_N\hat{N}|\Phi_q\rangle = 0.$$

In this equation, (i) Φ_q is the quasiparticle (qp) vacuum, (ii) $\hat{H}$ is the many-body nuclear Hamiltonian

$$\hat{H} = \sum_{i=1}^{A} T_i + \tfrac{1}{2}\sum_{i\neq j} v_{ij},$$

where T_i is the kinetic energy of the ith nucleon, and v_{ij} the finite range density-dependent force of Gogny and co-workers [32], (iii) $\hat{Q}_{20}$ and $\hat{Q}_{22}$ are external field operators which generate axial and triaxial quadrupole deformations, respectively, and (iv) $\hat{Z}$ and $\hat{N}$ are the proton and neutron numbers, respectively.

Finally, the Lagrange multipliers λ_i are determined by the constraints

$$\langle\Phi_q|\hat{Q}_{2i}|\Phi_q\rangle = q_{2i}$$

and

$$\langle\Phi_q|\hat{Z}(\text{or }\hat{N})|\Phi_q\rangle = Z \text{ (or } N).$$

Once the constrained HFB equations are solved, the potential energy surface is defined as

$$V(q) = \langle\Phi_q|\hat{H}|\Phi_q\rangle, \tag{1}$$

where the notation q=(q_{20}, q_{22}) is used. Since q_{20} and q_{22} are directly related to the Bohr coordinates β and γ, the potential energy surface (1) may also be expressed as V(β,γ).

In the second step, the dynamical states (i.e., the ground state and excited levels) are sought as

$$|\Psi\rangle = \int f(q)|\Phi_q\rangle dq,$$

where the superposition amplitude $f(q)$ is solution of the Griffin-Hill-Wheeler equation [33]

$$\int [H(q,q') - EI(q,q')]f(q')dq' = 0. \tag{2}$$

In this equation, $H(q,q') = \langle\Phi_q|\hat{H}|\Phi_{q'}\rangle$ is the nuclear kernel, $I(q,q') = \langle\Phi_q|\Phi_{q'}\rangle$ the overlap kernel, and E the energy.

In the third (and final) step, it is assumed that $I(q,q')$ is a Gaussian shape. Under this so-called Gaussian overlap approximation [30], Eq. (2) can be transformed into a second-order differential equation and expressed in the laboratory system,

$$\hat{\mathcal{H}}g(q) = Eg(q),$$

where

$$\hat{\mathcal{H}} = -\frac{\hbar^2}{2}\sum_{i,j}\frac{\partial}{\partial q_i}[M^{-1}(q)]_{ij}\frac{\partial}{\partial q_j} + \mathcal{V}(q) \tag{3}$$

is the collective Hamiltonian, $g(q)$ the Gauss transform of $f(q)$, and $\mathcal{V}(q)$ the potential energy surface corrected for zero-point energy $\Delta V(q)$ [i.e., $\mathcal{V}(q) = V(q) - \Delta V(q)$]. This correction term as well as the collective masses B_{ij} ($i,j = 0,2$) and moments of inertia J_i ($i = 1,3$), which completely define the tensor M_{ij}, are calculated in the cranking approximation [34].

$\hat{\mathcal{H}}$ is formally identical to the Bohr Hamiltonian considered by Kumar and Baranger [35]. Its eigenstates may be expressed in terms of the coordinates (β,γ),

$$|IM\rangle = \sum_{K=0}^{I} g_K^I(\beta,\gamma)\ |IMK\rangle.$$

Here, $|IMK\rangle$ is a normalized combination of Wigner rotation matrixes, with M and K as projections of the angular momentum I onto the third axis in the laboratory and inertia frames, respectively. Furthermore, $g_K^I(\beta,\gamma)$ is the vibration amplitude. It is such that the probability density

$$\rho^I(\beta,\gamma) = \sum_K |g_K^I(\beta,\gamma)|^2\mu(\beta,\gamma), \tag{4}$$

with $\mu(\beta,\gamma)$ as the metric of $\hat{\mathcal{H}}$, is normalized over the sextant $S_1 = \{\beta \geq 0\ ;\ 0° \leq \gamma \leq 60°\}$. Detailed discussions on the symmetry properties of $\hat{\mathcal{H}}$ may be found in Ref. [35].

To make complete our description of the nuclear states, we define the root mean square (rms) deformations $\beta_{\rm rms}$ and $\gamma_{\rm rms}$ through [36]

$$\beta^2_{\rm rms} = \langle IM|\beta^2|IM\rangle,$$

$$\beta^3_{\rm rms}\cos 3\gamma_{\rm rms} = \langle IM|\beta^3\cos 3\gamma|IM\rangle.$$

The only ingredient used in our set of calculations is the Gogny force. With it, pairing correlations are handled in a fully microscopic way requiring no additional parameters [32]. The collective Hamiltonian (3) is parameter free. This feature is in contrast with that of phenomenological collective models [25,35,37].

A. Potential energy surfaces

The PES calculations are shown in Fig. 1. A feature common to all isotopes is the existence of a minimum at small oblate deformation ($\beta \sim -0.15$). For ^{184,186}Hg, there exists another minimum at large prolate deformation ($\beta \sim 0.3$). This minimum is triaxial for ^{186}Hg ($\beta_{\rm min} = 0.29$, $\gamma_{\rm min} = 12°$) whereas it is axial for ^{184}Hg ($\beta_{\rm min} = 0.30$, $\gamma_{\rm min} = 0°$). Furthermore, these PES minima in both isotopes have comparable magnitude, and are separated by a triaxial barrier at most 1.2 MeV high. These results are consistent with earlier PES predictions for light Hg isotopes [19–24].

As one moves to heavier isotopes, the prolate minimum jumps up to $\beta \sim 0.55$, a broad plateau develops in ^{188}Hg at normal deformation (i.e., $\beta \sim 0.3$ and γ between 5° and 20°), and the triaxial barrier completely disappears in ^{188,190}Hg. At this stage it should be pointed out that a PES shoulder (or shallow minimum) is predicted at small prolate deformation ($\beta \sim 0.10$) for ^{190}Hg. This result is in good agreement with axial PES calculations reported by Zhang and Hamilton [27]. However, this shallow minimum does not secure the actual existence of a secondary PES minimum since no triaxial barrier exists between the absolute minimum predicted at oblate deformation and the shoulder at weak prolate deformation. Thus a simple inspection of the PES landscapes shown in Fig. 1 suggests an abrupt transition at A=188, between nuclei showing shape coexistence at normal deformations (^{184,186}Hg) and heavier isotopes (^{190}Hg and also ^{192,194}Hg; see Ref. [38]) in which coexistence takes place between normal and superdeformed (SD) shapes. It is worth noting that the coexisting bands observed [18] in ^{188}Hg at normal deformation do not seem obviously correlated to the topology of $V(\beta,\gamma)$ calculated for this isotope. This last remark makes the point that collective properties of complex nuclei do not exclusively depend upon PES landscapes, and that solutions of the collective Hamiltonian have to be considered.

B. Level schemes

The collective levels with $I \leq 6$ predicted for ^{190}Hg, ^{188}Hg, and ^{186}Hg have been classified into bands shown in Figs. 2, 3, and 4, respectively. It is difficult to organize these bands according to the main wave function K components because many excited states show K mixing. This is why the band structures have mainly been established from reduced transition probabilities $B(E2; I_i \rightarrow$

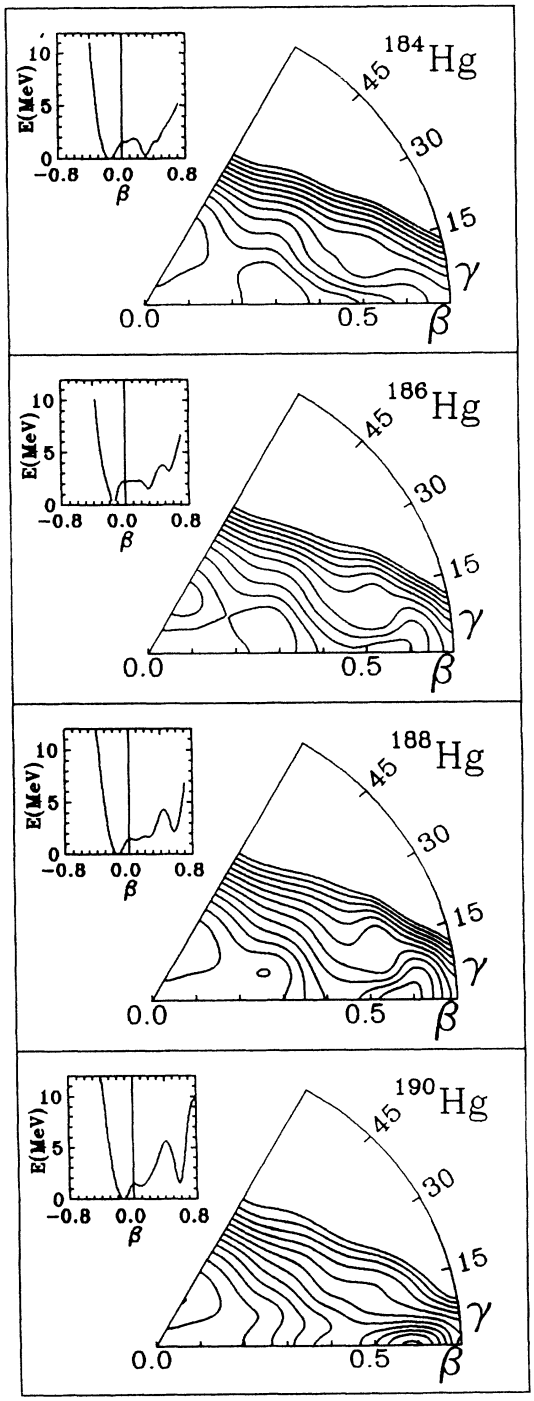

FIG. 1. Potential energy surfaces $V(\beta,\gamma)$ calculated for ^{184,186,188,190}Hg from our constrained HFB calculations. Zero point energies are included. Contours are separated by 1 MeV. Insets are cuts across the PES's along $\gamma = 0°$ and $\gamma = 60°$.

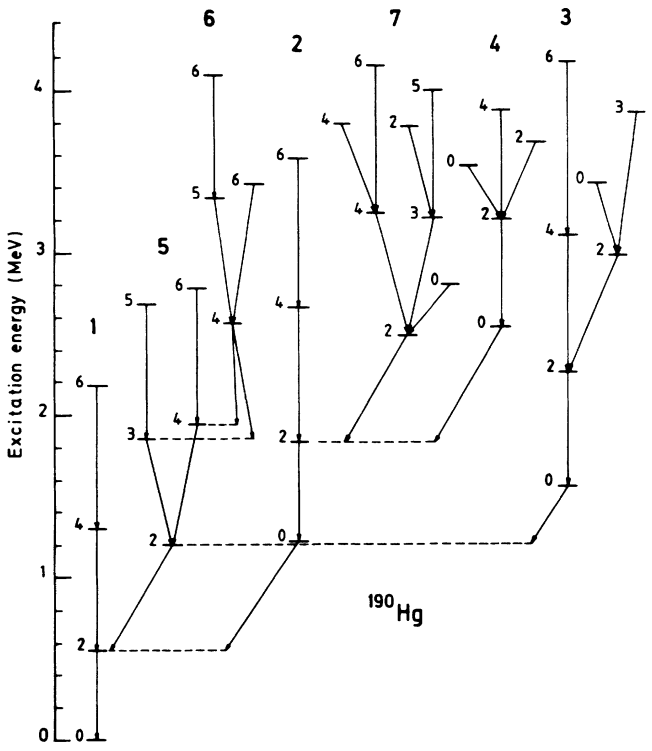

FIG. 2. Predicted positive-parity levels at low spins and excitation energies in ^{190}Hg. Band structure has been established using the largest reduced transition probabilities shown as arrows between two states. Labels are given at the top of bands.

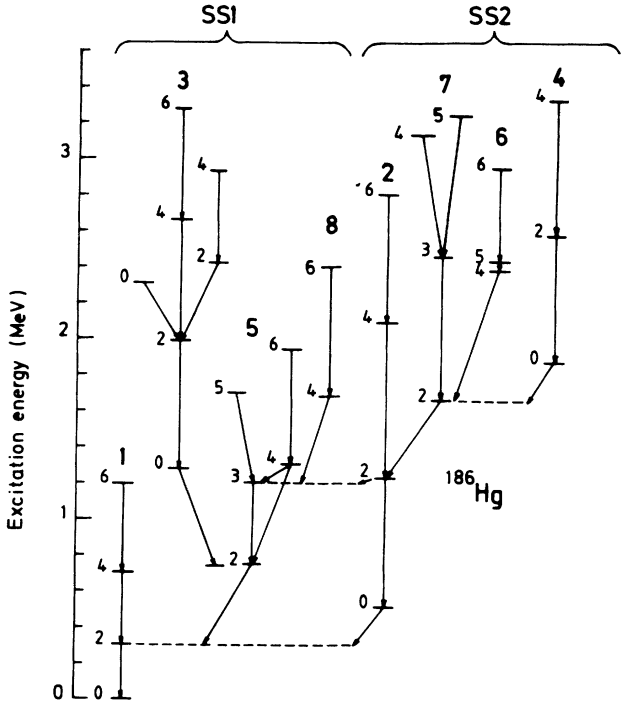

FIG. 4. Predicted positive-parity levels at low spins and excitation energies in ^{186}Hg. The bands are organized in two substructures SS1 and SS2. From left to right are successively shown the deformed bands (labeled as 1, 3, 5, and 8) and the weakly deformed bands (labeled as 2, 7, 6, and 4). For other details, see caption of Fig. 2.

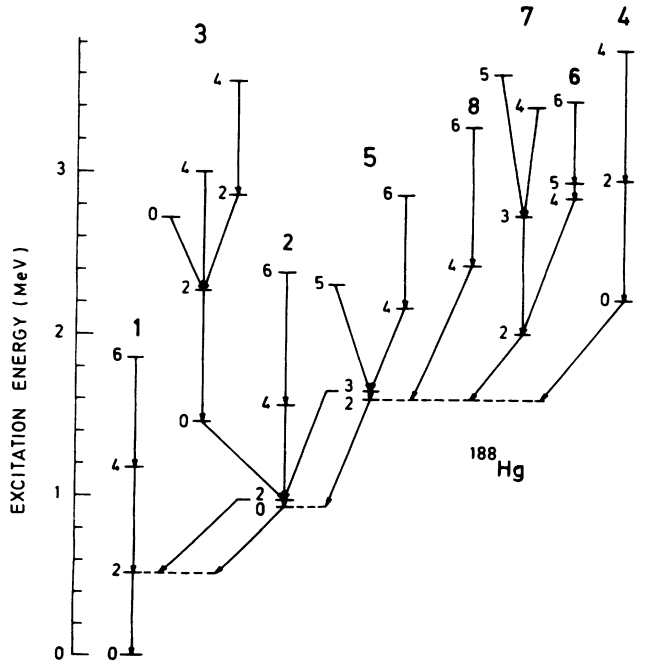

FIG. 3. Predicted positive-parity levels at low spins and excitation energies in ^{188}Hg. For more details, see caption of Fig. 2.

I_f) calculated for electric quadrupole ($E2$) transitions between any initial (I_i) and final (I_f) states using effective $E2$ transition operators defined in Refs. [35] and [36]. Only the main γ-decay paths are shown in Figs. 2–4.

1. Level predictions for ^{190}Hg

The quasirotational bands are shown in Fig. 2 where band 1 is the g.s. band. The next sequence of levels with $I = (2,(3,4),(5,6))$ is the quasi-γ-band (i.e., band 5), upon which is built a quasi-$\gamma\gamma$-band (i.e., band 6). Then follows the $I = (0,2,4,6)$ sequence which is the quasi-β-band (i.e., band 2). Within the language of the interacting boson model [39], the whole spectrum including the seven bands formally resembles that of a transitional SU(3)$\rightarrow$ O(6) nucleus.

2. Level predictions for ^{188}Hg

As compared to ^{190}Hg, the isotope ^{188}Hg displays a slightly more deformed shape in its ground state (Fig. 3). It also shows rather different band structures that directly stem from the marked differences between the PES's for the two isotopes (Fig. 1). Considerable K mixing has been found in the predicted levels of ^{188}Hg, rendering only plausible the classification into bands. A test

intended to sustain the validity of this band structure consisted in performing sensitivity calculations in which the collective masses B_{ij} and moments of inertia J_i are varied separately. Without any coupling between rotations and vibrations, one expects that (i) increasing J_i's would make the $I = (0, 2, 4, 6)$ sequences looking more rotational, and (ii) increasing $B_{i,j}$'s would shift down in energy the $I = (0, 2, 4, 6)$ and (2,3,4,5,6) sequences. The sensitivity tests have been performed by solving the collective Hamiltonian (3) in which the B_{ij}'s and J_i's are separately increased by 40%. As expected, increasing the B_{ij}'s pulls down the excitation energy E_x of the $K = 0$ excited bands (i.e., bands 2, 3, and 4). Moreover, this lowering gets more important in magnitude as E_x increases. For instance, E_x for band 2 is now 100 keV lower than the excitation energy shown in Fig. 3, while the lowering of band 4 amounts to 400 keV. All the other excited bands (i.e., bands 5, 6, 7, and 8) also get shifted to lower excitation energies but the lowering is not as strong as it is for bands 2 and 4, which means that they do not have a plain vibrational character. On the other hand, the 40% increase in J_i's propagates on the band structure predictions as follows: (i) the heads of bands 2–4 are unaltered, (ii) all the bands look more deformed (as expected), and (iii) the differences in energy between the 2^+ and 0^+ members of band 2 and between the 3^+ and 2^+ members of band 5 flip their signs. Both sensitivity tests illuminate the complex interplay that takes place between vibrations and rotation in ^{188}Hg.

3. *Level predictions for ^{186}Hg*

Among the neutron-deficient Hg isotopes under study, ^{186}Hg is certainly the nucleus showing maximum K mixing in its predicted collective states. None of these levels have a dominant vibrational or rotational character. Using sensitivity tests similar to those described above

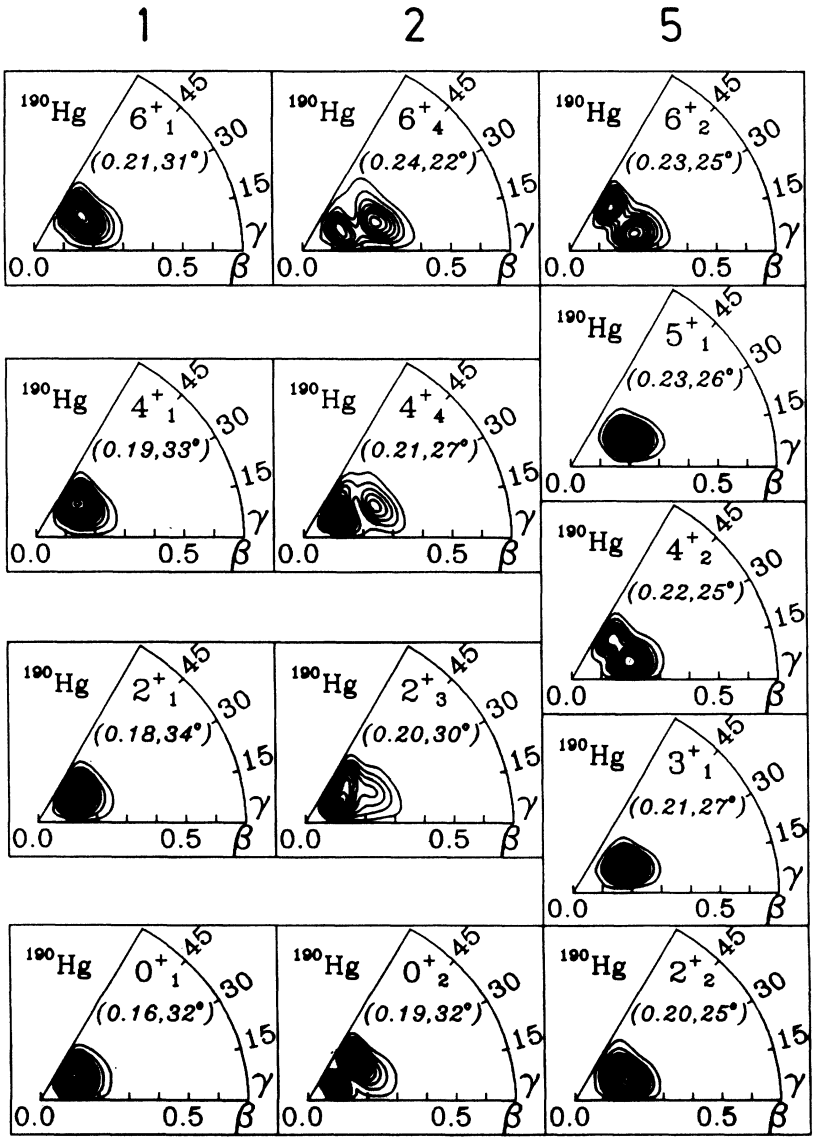

FIG. 5. ^{190}Hg. Probability densities ρ^I over the (β,γ) plane for members of the ground-state band (band 1), quasi-β-band (band 2), and quasi-γ-band (band 5).

for ^{188}Hg, it has, however, been possible to organize the ^{186}Hg levels into quasirotational bands. As shown in Fig. 4, the main decay paths suggest that bands 1–8 belong to two distinct substructures (SS's): SS1 includes bands 1, 3, 5, and 8, while SS2 is made up with bands 2, 4, 6, and 7. The level spacings inside the various bands suggest that SS1 is more deformed than SS2 (compare bands 1 and 2, bands 5 and 7, etc.). Also, each substructure displays a quasi-γ-band and other sequences of excited states. All these results point to the fact that shape coexistence takes place not only between the g.s. and first excited bands (i.e., bands 1 and 2) but also between the quasi-γ-bands (i.e., bands 5 and 7). This picture is consistent with the existence of two minima in the potential energy surface of ^{186}Hg (see Fig. 1).

4. Level predictions for ^{184}Hg

Coexistences between $K = 0$ bands and between γ bands are also predicted for ^{184}Hg. The bandhead levels (not shown here) have excitation energies similar to those displayed in Fig. 4 for ^{186}Hg.

C. Probability densities for ^{190}Hg

The probability densities $\rho^I(\beta, \gamma)$ are shown in Fig. 5 for the first members of the g.s. band (band 1), quasi-β-band (band 2), and quasi-γ-band (band 5) in ^{190}Hg. The topology of these densities together with rms deformations ($\beta_{\rm rms} \sim 0.20$) much larger than the deformation of the PES minimum ($\beta_{\rm min} = 0.13$; see Fig. 1) obviously indicate large dynamical triaxiality as well as softness with respect to the elongation axis (i.e., β coordinate). These properties are favorable to the formation of β and γ bands at low excitation energy. On the other hand, none of the probability density distributions is suggestive of shape coexistence in ^{190}Hg.

III. EXPERIMENTS

Among all the model predictions described above, those of importance for guiding the measurements and data analyses to be discussed below for ^{190}Hg and ^{186}Hg are the following: (i) Quasi-γ-bands should exist at low excitation energy in both Hg isotopes, (ii) a coexistence between two quasi-γ-bands is expected to show up in ^{186}Hg, and (iii) a quasi-β-band should exist at low excitation energy in ^{190}Hg.

A. Methods

The excited levels of ^{190,186}Hg have been studied from β^+/EC decays of ^{190}Tl^{g,m} and ^{186}Tl^{g,m} using the ISOCELE facility [40]. Thallium isotopes were produced in ^{197}Au(^{3}He, xn)Tl reactions using the 280 MeV ^{3}He beam delivered by the Orsay synchrocyclotron [$I(^3\text{He}) \sim 2\ \mu$A]. The radioactive ions extracted from the ion source were then mass separated, collected on a Mylar-aluminum tape, and automatically transported to the detection setup.

In the study of ^{190}Hg, the setup consisted of three hyperpure (HP) Ge n-type coaxial detectors placed approximately 5 cm from the radioactive source: (i) two detectors [full width at half maximum (FWHM) =1.9 keV at 1.33 MeV and 18% efficiency] covering a 30 keV–3 MeV energy range and (ii) one detector (FWHM = 2.3 keV at 1.33 MeV and 73% efficiency) covering a 100 keV–6 MeV energy range. γ-γ-t coincidence events were recorded in event-by-event mode on magnetic tapes. In order to keep a good energy resolution over these large energy ranges, coincidence data were digitized with an 8192 conversion gain. As an example, a total of 150×10^6 events were obtained in the prompt coincidence matrix for the range 100 keV–3 MeV. To illustrate this high statistics, the γ-ray spectrum obtained in coincidence with the 658 keV transition is shown in Fig. 6. Despite the weakness in intensity of this transition (see Table I), the 506 keV γ line is clearly observed in the coincidence spectrum.

In the study of ^{186}Hg, the setup consisted of four Ge(HP) n-type coaxial detectors (FWHM = 1.9 keV at 1.33 MeV and 18% efficiency) placed approximately 13 cm from the radioactive source. They covered a 20–1500 keV energy range. The different angles subtended by the counteraxes were chosen such that experimental values of the angular correlation function

$$W(\theta) = 1 + A_2 P_2(\cos\theta) + A_4 P_4(\cos\theta)$$

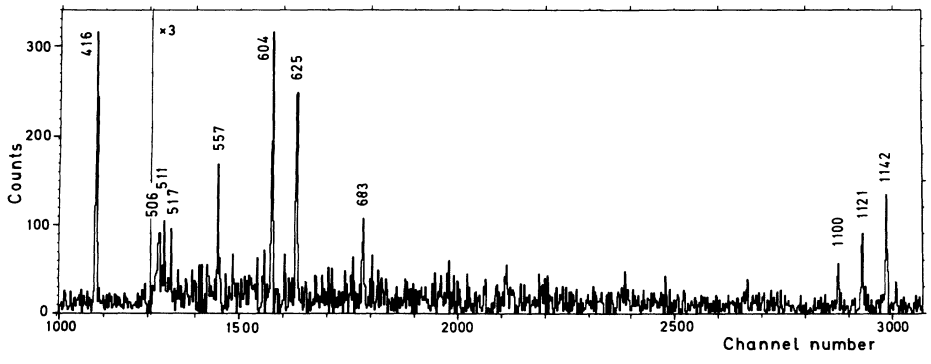

FIG. 6. Coincidence γ-ray spectrum for gate set on the 658 keV transition in ^{190}Hg. Energies are in keV.

can be measured at six angles θ: 7°, 30°, 50°, 57°, 80°, and 87°. The level scheme of ^{186}Hg has been built from coincidence relationships observed between γ rays analyzed in a 4096 × 4096 channel coincidence matrix with all the events (the prompt coincidence matrix contained a total of 100 × 10^6 events). For the angular correlation analysis, the data have been sorted into six γ-γ (θ) matrixes each including approximately 40 × 10^6 events, and $W(\theta)$ values have been obtained for different cascades. Detailed description of the method can be found in Ref. [41].

B. Experimental results for ^{190}Hg

An extended level scheme has been built from the γ-γ coincidence relationships. Besides the g.s. band levels

TABLE I. γ-decay properties of ^{190}Hg positive-parity levels populated in the ^{190}Tl decay.

Initial level		Final level		Gamma ray		
E_i (keV)	I^π	E_f (keV)	I^π	E_γ (keV)[a]	I_γ[b]	$B(E2)$[c]
416.4	2^+	0.0	0^+	416.4	1000	100
1041.8	4^+	416.4	2^+	625.4	817	100
1773.0	6^+	1041.8	4^+	731.2	345	100
1100.0	2^+[d]	416.4	2^+	683.5	63	94
		0.0	0^+	1100.0	40	6
1558.7	$2^+,3^\pm,4^+$	1100.0	2^+	458.8	10	70
		1041.8	4^+	516.8	7	27
		416.4	2^+	1142.4	40	3
1657.1	$2^+,3^\pm,4^+$	1100.0	2^+	557.1	57	72
		1041.8	4^+	615.2	36	28
		416.4	2^+	1241.2	6.1	0.1
2163.0	$4^+,5^\pm,6^+$	1773.0	6^+	390.1	2.0	36
		1657.1		506.0	5.9	29
		1558.7		604.3	17	34
		1041.8	4^+	1120.9	8.7	0.7
2201.3	$4^+,5^\pm,6^+$	1773.0	6^+	428.1	3.0	15
		1657.1		543.8	54	85
		1041.8	4^+	1159.7	5.1	0.2
2821.7	$4^+,5^\pm,6^\pm,7^+$	2201.3		620.4	1.0	16
		2163.0		658.7	7.3	84
1850.8	$2^+,3^\pm,4^+$	1100.0	2^+	750.8	12.0	69
		1041.8	4^+	808.8	7.9	31
		416.4	2^+	1434.7	1.4	0.003
2342.9	$4^+,5^\pm,6^+$	2201.3		142.7	2.2	99
		1850.8		492.1	4.7	0.5
		1773.0	6^+	569.9	3.0	0.1
		1657.1		685.8	6.0	0.1
		1041.8	4^+	1300.8	1.6	0.001
2365.4	$4^+,5^\pm,6^+$	1975.4	4^+	390.1	2.0	67
		1850.8		514.5	1.8	15
		1773.0	6^+	592.6	4.0	16
		1041.8	4^+	1323.4	17	1
1278.6	0^+[e]	416.4	2^+	862.2	1.0	100
1571.4	2^+[e]	1041.8	4^+	530.0	<0.3	<74
		416.4	2^+	1155.0	4.4	>22
		0.0	0^+	1571.1	3.4	>4
1975.4	4^+[e]	1571.4	2^+	403.9	2.0	95
		1041.8	4^+	933.8	4.6	4
		416.4	2^+	1559.1	12	0.7
2510.1	6^+[e]	1975.4	4^+	534.7	4.0	83
		1773.0	6^+	737.1	4.0	16
		1041.8	4^+	1468.4	4.8	0.7

[a] $\Delta E_\gamma \leq 0.2$ keV if $I_\gamma > 100$, and 0.3 keV otherwise.
[b] Intensities normalized to I_γ (416 k eV) = 1000.
[c] Branching ratios normalized to $\sum_f B(E2; I_i \rightarrow I_f) = 100$.
[d] Taken from Ref. [43].
[e] Taken from Ref. [28].

observed up to spin 8^+ and negative-parity states identified up to spin 10^- [42], about 100 levels have been identified up to 4 MeV excitation energy. The γ rays linking these levels have intensities down to 0.5 part in 1000 disintegrations.

Only the levels relevant to the present discussion are presented in Table I; these are the following: (i) The first four members of the g.s. band. (ii) The six levels located at 1100.0, 1558.7, 1657.1, 2163.0, 2201.3, and 2821.7 keV that can be organized into a quasirotational band from their decay modes. The band head (E_x = 1100.0 keV) partly decays to the ground state via an $E2$ transition [43]. It has spin and parity $I^\pi = 2^+$, and may be the head of the quasi-γ-band we are searching for. (iii) The levels located at 1850.8 and 2342.9 keV which are linked to the quasi-γ-band, and the 2365.4 keV level which decays to the 1850.8 keV excited state. (iv) A second excited band consisting of states located at 1278.6, 1571.4, 1975.4, and 2510.1 keV. This band is identical to that recently reported by Kortelahti *et al.* [28], but we do not observe the 293 keV transition deexciting the 1571.4 keV level towards the 1278.6 keV excited state. Furthermore, the relative intensities that we have found for the γ-ray transitions deexciting the other levels in the band (see Table I) are not completely in agreement with the previous measurements [28].

It is worth noting that the levels in the excited bands are not highly populated from the ^{190}Tl decay. Taking the intensity of the $2^+ \rightarrow 0^+$, 416.4 keV transition as reference (see Table I), the relative γ-ray intensities observed in our measurements are less than 6.5% for the first excited band and less than 1.2% for the second.

C. Experimental results for ^{186}Hg

In this nucleus, two rotational bands with different moments of inertia have been found [8–11]. The first one

TABLE II. γ-decay properties of ^{186}Hg positive-parity levels populated in the ^{186}Tl decay.

Initial level		Final level		Gamma ray		
E_i (keV)	I^π	E_f (keV)	I^π	E_γ (keV)[a]	I_γ[b]	$B(E2)$[c]
405.2	2^+	0.0	0^+	405.2	100	100
1080.0	4^+[d]	807.7	4^+	271.9	0.9	70
		620.7	2^+	459.1	3.2	18
		405.2	2^+	675.1	14	12
1677.4	(6^+)	1080.0	4^+	597.3	5.2	97
		807.7	4^+	869.7	1.0	3
620.7	2^+[d]	405.2	2^+	215.5	5.7	99.9
		0.0	0^+	621	~0.7	0.1
807.7	4^+	620.7	2^+	186.7	2.5	70
		405.2	2^+	402.5	49	30
1164.4	6^+	807.7	4^+	356.7	32	100
1096.4	2^+[e]	523	0^+	573.2	1.7	60
		405.2	2^+	691.2	~3	40
1433.3	$2^+,3^\pm,4^+$	1096.4	2^+	337.1	~0.3	69
		807.7	4^+	625.5	2.1	22
		620.7	2^+	812.7	3.3	9
1659.2	$2^+,3^\pm,4^+$	1096.4	2^+	562.8	1.0	28
		1080.0	4^+	579.2	~3	72
1868.1	$4^+,5^\pm,6^+$	1433.3		434.7	~2	87
		1164.4	6^+	704	~2	8
		1080.0	4^+	788.1	2.9	5
2129.9		1433.3		696.6	0.5	100
2137.6	$2^+,3^\pm,4^\pm,5^\pm,6^+$	1659.2		478.6	~1	94
		1080.0	4^+	1057.6	3.3	6
2211.2	$2^+,3^\pm,4^\pm,5^\pm,6^+$	1433.3		777.9	1.4	97
		1080.0	4^+	1131.3	0.3	3
2267.7		1868.1		399.6	0.5	100
2348.6	$6^+,7^\pm,8^+$	1906.0		442.5	0.5	33
		1868.1		480.6	1.5	64
		1588.4	8^+	760.1	0.6	3
2427.5	$4^+,5^\pm,6^\pm,7^\pm,8^+$	1868.1		559.7	0.8	92
		1677.4	(6^+)	749.8	0.3	8

[a] $\Delta E_\gamma \leq 0.2$ keV if $I_\gamma > 10$, and 0.3 keV otherwise.
[b] Intensities normalized to I_γ (405 keV) = 100.
[c] Branching ratios normalized to $\sum_f B(E2; I_i \rightarrow I_f) = 100$.
[d] Spin value [10] confirmed from angular correlation measurements (present work).
[e] Spin value determined from angular correlation measurements (present work).

(i.e., the g.s. band) is characteristic of that for a weakly deformed nucleus, while the second is typical of that for "normally deformed" nuclei in the $A = 180$–190 mass region. In the present decay measurements, states with spins up to 8^+ and 10^+ were populated in the first and second bands, respectively. Only those with $I \leq 6$ are given in Table II.

Among the new excited states which were identified the one located at 1096.4 keV is $I = 2$, a spin value assigned from angular correlation analysis of the 691 keV-405 keV cascade. This analysis has been conducted in three steps, as illustrated in Fig. 7. First, the coefficients $A_2^{\text{expt}} = -0.288 \pm 0.124$ and $A_4^{\text{expt}} = +0.474 \pm 0.167$ were determined from a least-squares fit to the measured $W(\theta)$ values [see Fig. 7(a)]. These values clearly indicate that $I = 2$ for the 1096.4 keV level. Next, the coefficients A_2 and A_4 were calculated for a 2(1,2)2(2)0 cascade [44] as a function of the mixing ratio δ [$\delta^2 = I_\gamma(E2)/I_\gamma(M1)$] for the 691 keV transition. As can be seen in Fig. 7(b), there exists an overlap between the measured and calculated A_2's and A_4's only for $\tan^{-1}\delta \sim 80°$. The inferred mixing ratio is $\delta = 5.7^{+2.0}_{-1.2}$, which means that the 691 keV transition has an $M1$ + 97% $E2$ multipolarity. Finally, the angular correlation function for the 2(1,2)2(2)0 cascade was obtained using the theoretical values $A_2 = -0.187$ and $A_4 = +0.316$ calculated using $\delta = 5.7$. This function is shown as solid curve in Fig. 7(c) where it is compared with the measured $W(\theta)$'s to illustrate the quality of our experimental results. The 2^+ ($E_x = 1096.4$ keV) level most likely is the head of the lowest quasi-γ-band, an interpretation also supported by the dominant $E2$ character found for the 691 keV transition linking this level with the first 2^+ excited state. Table II includes its γ-decay properties as well as those for other newly discovered levels showing strong links with it.

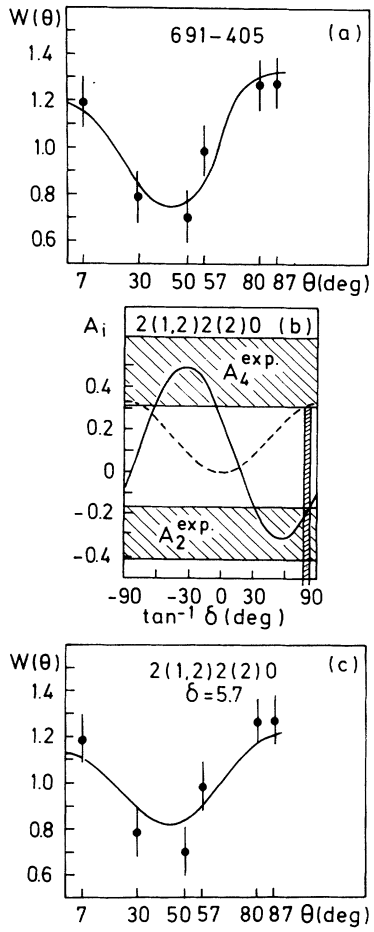

FIG. 7. Angular correlation function for the 691-405 keV γ-ray cascade in ^{186}Hg. (a) Comparison between present experimental values (dots) and the function (solid curve) determined from a least-squares fit to the data. (b) Theoretical A_2 (solid curve) and A_4 (dashed curve) values calculated as a function of $\tan^{-1}\delta$ for a 2(1,2)2(2) 0 cascade, with δ as mixing ratio [i.e., $\delta^2 = I_\gamma(E2)/I_\gamma(M1)$]. The two wide hatched areas correspond to experimental A_i values determined from the least-squares fit, and the narrow hatched area is for the overlap between experimental and theoretical A_2 and A_4 values. (c) Comparison between our measurements (dots) and the calculations (solid curve) performed using $\delta = 5.7$ as extracted from the curves shown in Fig. 7(b). For more details, see text.

IV. BAND IDENTIFICATIONS AND PROPERTIES

Quasirotational bands built from the γ-decay patterns observed in the present measurements are now compared with our theoretical predictions. As can be seen in Figs. 8 and 9, the predicted moments of inertia are approximately 30% lower than those deduced from measurements. This feature stems from using the cranking approximation [34], as already discussed in Ref. [46].

A. Band structure for ^{190}Hg

Our model calculations shown in Fig. 2 suggest that the 4^+ member of the g.s. band, the 0^+ head of the quasi-β-band (i.e., band 2), and the 2^+ head of the quasi-γ-band (i.e., band 5) have similar excitation energies (i.e., $E_x \sim 1200$ keV). These predicted levels have experimental counterparts: the first 4^+ level located at 1041.8 keV, the second 0^+ at 1278.6 keV, and the second 2^+ at 1100.0 keV, respectively (see Table I). The third 2^+ level observed at 1571.4 keV very likely is a member of the quasi-β-band despite the weak intensity of the 292.8 keV $2_3^+ \rightarrow 0_2^+$ transition which is mentioned in Ref. [28] but not observed in our work. Therefore, the observed bands can be identified as the predicted bands 1, 2, and 5 (see Fig. 8). Usually, the level density in a γ band is neither uniform nor distributed according to the strong coupling scheme: The band members go pairwise. For ^{190}Hg the sequence of spins 2^+, (3^+, 4^+), (5^+, 6^+), and 7^+ is observed. Our predictions are in rather good agreement with this experimental pattern (see Fig. 8).

Three additional $\pi = +$ excited states observed at 1850.8, 2342.9, and 2365.4 keV are worth mentioning.

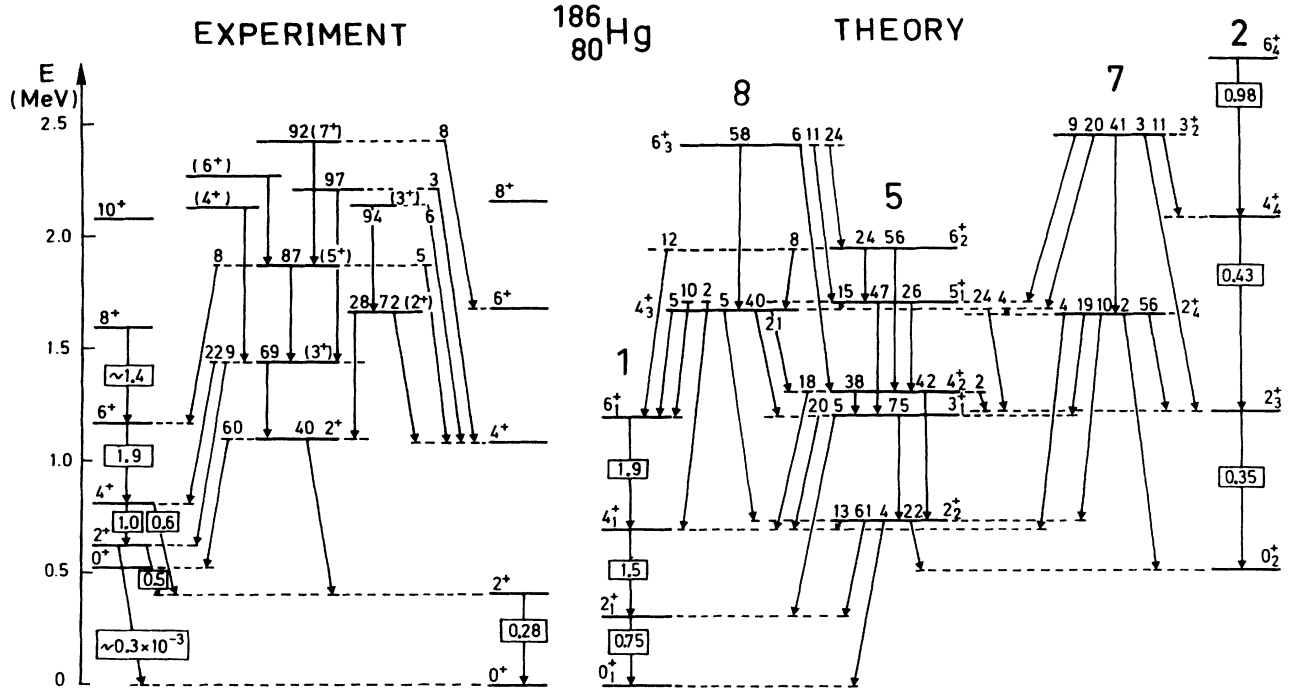

FIG. 8. Positive-parity levels of ^{190}Hg at normal deformation and low excitation energy. Comparison between present theoretical predictions and experimental results obtained at ISOCELE from the β^+/EC decay of ^{190}Tl^{g,m}. For both experimental and theoretical results, and from left to right, the levels are organized in quasirotational bands: g.s., γ, and β bands. Relative $E2$ branching ratios [normalized to $\sum_f B(E2; I_i \to I_f) = 100$] are shown on top of levels in the γ and other excited bands. Absolute $B(E2)$ values (in $e^2\,b^2$ units) predicted in this work are inserted in boxes.

The first one (E_x = 1850.8 keV) mainly decays towards the 2^+ (E_x = 1100 keV) level previously identified as the γ bandhead; it may be interpreted as the 4^+ head of a $\gamma\gamma$ (i.e., two-phonon) vibrational band. The second (E_x = 2342.9 keV) which decays towards this 4^+ state may be the 5^+ (or 6^+) member of the $\gamma\gamma$ band. The third excited state (E_x = 2365.4 keV) is tentatively identified as the 4^+ member of band 7. These three levels are also shown in Fig. 8.

Comparisons between experimental results and theoretical predictions have been extended to reduced transition probabilities. Some are shown in Fig. 8 as branching ratios normalized to $\sum_f B(E2; I_i \to I_f) = 100$. It is worth noting that the predictions are in excellent agreement with the measurements for the γ band. On the other hand, our theory does not predict properly the branching ratios measured for the other excited states in the vicinity of (or above) the pairing gap. This weakness is not surprising since our theoretical model is based on the adiabatic approximation in which the two quasiparticle (2qp) excitations indeed are ignored.

In summary, the three excited bands observed in ^{190}Hg can be interpreted unambiguously as quasi β- , γ-, and $\gamma\gamma$-bands.

B. Band structure for ^{186}Hg

The g.s. band observed in this Hg isotope (see Fig. 9) is clearly associated with a weakly deformed shape, while the excited $K = 0$ band indicates large but normal deformation. In contrast, the g.s. band predicted here is normally deformed, whereas the $K = 0$ excited band is weakly deformed (see Figs. 4 and 9). This inversion in excitation energy between the predicted $K = 0$ yrast and yrare bands, and more generally between the substructures SS1 and SS2 shown in Fig. 4, is not presently understood. This feature of our collective model predictions for ^{186}Hg is in sharp contrast with plain expectations based on the observation of an absolute PES minimum at small (oblate) deformation. Improvements in our predictions may require the projection of HFB solutions on good particle numbers and breaking the left-right symmetry so far imposed onto the triaxial mean field calculations, studies out of the scope of the present work.

However, our predictions are very useful to assist the experimental identification of coexisting γ bands in ^{186}Hg. This may be accomplished in one's imagination by shifting down in energy the whole substructure SS2

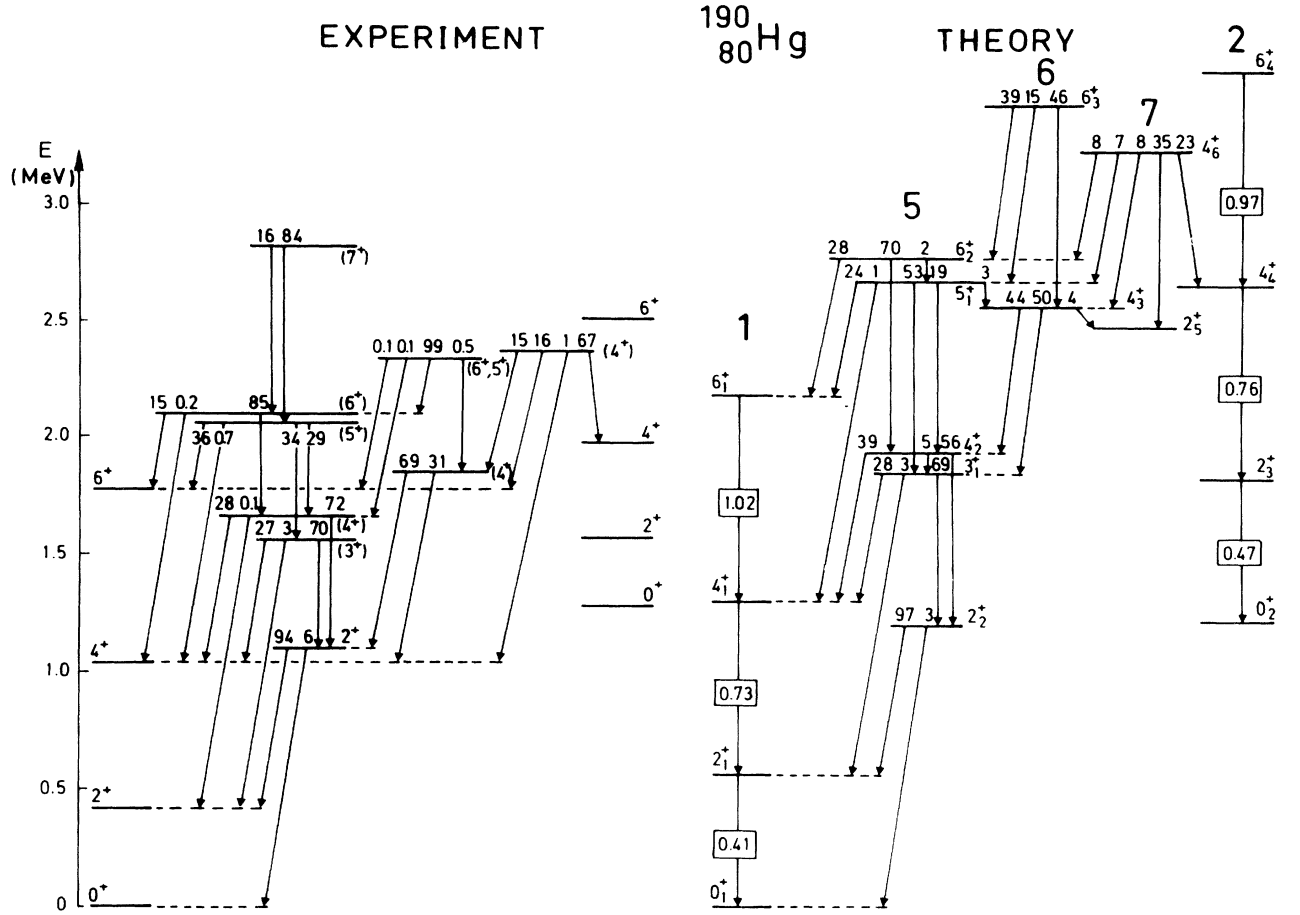

FIG. 9. Positive-parity levels of ^{186}Hg at low excitation energy. Comparison between present theoretical predictions and experimental results obtained at ISOCELE from the β^+/EC decay of ^{186}Tl^{g,m}. Experimental $B(E2)$ values are taken from Refs. [9] and [45]. From left to right in the "experiment" panel are shown (i) the normally deformed $K = 0$ band, (ii) the first γ band [made up with the 2^+(1096.4 keV), (3^+)(1433.3 keV), (5^+)(1868.1 keV), and (7^+)(2427.5 keV) levels], (iii) the second γ band [made up with the (2^+)(1659.2 keV) and (3^+)(2137.6 keV) levels], and (iv) the weakly deformed $K = 0$ band. The "theory" panel is organized in a similar manner. Note that the 4_2^+ and 6_2^+ levels predicted in the first γ band are shown although their experimental counterparts have not presently been observed. For more details on the absolute and relative $B(E2)$ values, see caption of Fig. 8.

shown in Fig. 4. For instance, a 1 MeV shift would artificially make band 2, the weakly deformed g.s. band, and band 1, the $K = 0$ excited band now located at $E_x \sim 500$ keV, figure close to the experimental excitation energy of this band. By the same token, bands 5, 6, 7, and 8 would show up as completely interwoven γ-vibrational bands, some decaying mainly to the g.s. band and others to the $K = 0$ excited band.

The excited states observed at $E_x = 1096.4$, 1433.3, and 1868.1 keV from our β^+/EC decay measurements display strong links and main decay paths to the deformed $K = 0$ band (see Table II). Since they also show (i) energy transitions similar to those for band 5, Fig. 9, and (ii) branching ratios in good agreement or consistent with the theoretical expectations, these levels are identified as the 2^+, 3^+, and 5^+ members of a γ band (i.e., band 5). The 2^+ head level of this band lies 573 keV above the 0^+ member of the deformed $K = 0$ band, a relative excitation energy (E_r) in fairly good agreement with $E_r = 736$ keV inferred from our predictions. The excited state at $E_x = 2427.5$ keV which mainly decays to the 5^+(1868.1 keV) level is tentatively assigned a spin 7^+; it is probably the last band 5 member that we are able to identify with some confidence.

Above the 2^+ γ bandhead is observed an excited state ($E_x = 1659.2$ keV) which mainly decays to the 4^+ member of the weakly deformed $K = 0$ band. This level may be identified as the 2^+ member of the coexisting γ band (i.e., band 7) we are searching for, and is shown in the right-hand side (RHS) of the "experiment" panel in Fig. 9. It has for its theoretical counterpart the 2_4^+ excited state shown in the RHS of the "theory" panel. As can be seen, this predicted 2_4^+ level mainly decays to the weakly deformed band. The level observed at $E_x = 2137.6$ keV

mainly decays to the (2^+) (E_x=1659.2 keV) excited state. Therefore it is tentatively identified as the $I = 3$ member of the second γ band (i.e., band 7).

We have also observed three other levels below 2.3 MeV, all decaying towards excited states of the γ bands. The first one located at E_x= 2129.9 keV decays only to the (3^+) level of the first γ band. It cannot be the 4^+ member of this band because its observed excitation energy is too high. On the other hand, it may be identified with the 4_3^+ level which mainly decays to the 3^+ member of the γ band (i.e., band 5 in the "theory" panel of Fig. 9). The second level decays only towards the (5^+) member of the first γ band. Its excitation energy E_x = 2267.7 keV is not too different from that predicted for the 6_2^+ member of the first γ band. In spite of that, this level cannot be identified with the 6_2^+ excited state because the $6^+ \rightarrow 4^+ \rightarrow 2^+$ cascade has not been observed in the first γ band. Instead, we have tentatively identified the level observed at E_x = 2267.7 keV with the next 6^+ (i.e., 6_3^+) state which is a member of the $\gamma\gamma$ band (i.e., band 8 in Fig. 9). The third level located at E_x = 2211.2 keV and another one (not shown in Fig. 9) at E_x = 2348.6 keV could be identified to none of the predicted states. Since they are observed at excitation energies above the pairing gap, their wave functions most likely have 2qp components that are not treated in our theoretical framework.

Although far from complete, the experimental information we have collected at low spin for bands labeled 5 and 7 in Fig. 9 strongly suggests that shape coexistence between quasi-γ-bands is observed for the first time in ^{186}Hg.

V. $B(E2)$ VALUES: SIGNATURE OF SHAPE EVOLUTIONS THROUGH THE ^{184,186,188,190}Hg ISOTOPES

All the results so far discussed clearly indicate that a shape evolution is taking place throughout the neutron-deficient Hg isotopes. This evolution is now studied and discussed for mass increasing from A = 184 to 190 by means of $E2$ reduced transition probabilities.

The $B(E2)$ values determined from previous lifetime measurements performed for excited states in ^{184}Hg [17], ^{186}Hg [8–11,45], and ^{188}Hg [18,45] are shown in Table III [the $B(E2)$ values for ^{186}Hg are also inserted into boxes; see Fig. 9]. As can be seen, the $E2$ rates measured for transitions in the g.s. bands are generally much weaker than those obtained for transitions in the excited $K = 0$ bands, collective properties adding considerable weight to the coexistence picture offered for these bands in ^{184,186}Hg. The $B(E2)$ values here predicted for in-band transitions in the ^{184,186}Hg coexisting $K = 0$ bands are in excellent agreement with the available measurements in spite of the energy inversion between the $K = 0$ bands.

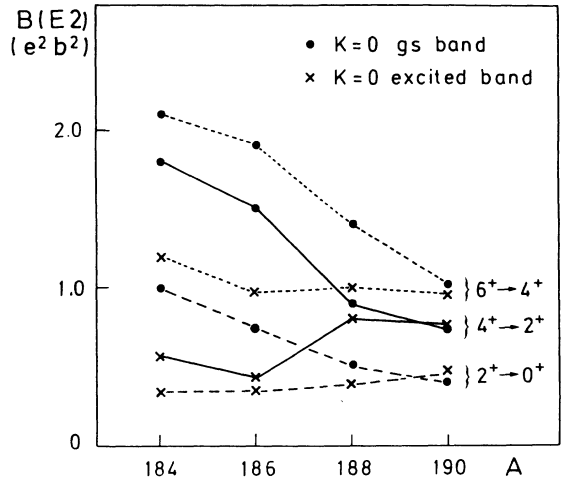

FIG. 10. Calculated $B(E2;I_i \rightarrow I_f)$ values for the lower two $K = 0$ bands predicted in ^{184,186,188,190}Hg. The variations of the $B(E2)$'s with A for the $6^+ \rightarrow 4^+$, $4^+ \rightarrow 2^+$, and $2^+ \rightarrow 0^+$ transitions are shown as dotted, solid, and dashed curves, respectively.

Taking advantage of this ability found in the present theoretical model to predict reliable $B(E2)$ values for transitions in the $K = 0$ bands, we now discuss the $B(E2)$ predictions for such bands to further characterize the shape evolution through the ^{184,186,188,190}Hg isotopes. As can be seen in Table III and Figs. 8–10, the in-band transitions for the two bands show increasing strengths with increasing spins. This can be explained by geometrical factors entering the calculated $B(E2)$ values and also by centrifugal stretching, a feature expected for

TABLE III. $B(E2)$ values (in $e^2\,b^2$) for the lower two $K = 0$ bands in ^{184,186,188}Hg. The experimental results are from Refs. [17,9,45]. Theoretical calculations are performed only for $I \leq 6$.

Band identification		^{184}Hg	^{186}Hg	^{188}Hg
Weakly deformed				
$2^+ \rightarrow 0^+$	expt.	0.39	0.28	0.4
	theor.	0.35	0.35	0.5
Normally deformed				
$4^+ \rightarrow 2^+$	expt.		1.0	
	theor.	1.8	1.5	
$6^+ \rightarrow 4^+$	expt.	2.1	1.9	
	theor.	2.1	1.9	
$8^+ \rightarrow 6^+$	expt.	2.2	~1.4	

these soft nuclei. We also note that the general trend in the $B(E2)$'s calculated for the $K = 0$ bands is a decrease in magnitude with increasing mass number, and that the difference between $B(E2)$ strengths for the $K = 0$ bands in a nucleus gradually decreases when moving from ^{184}Hg to ^{188}Hg and vanishes for ^{190}Hg (see Fig. 10). The first property obviously is related to the proximity of the $N = 126$ shell closure. The second indicates that, at normal deformation, shape coexistence phenomena end abruptly at ^{190}Hg. This result gives additional weight to our interpretation that the $K = 0$ excited band in ^{190}Hg is a quasi-β-band.

To complete this discussion, let us mention that ^{188}Hg plays a pivotal role in the shape evolution through the ^{184,186,188,190}Hg isotopes.

VI. SUMMARY

From our β^+/EC decay measurements, new collective bands have been observed in ^{186}Hg and ^{190}Hg. These structures found at low excitation energy are identified as quasi-γ-bands. Their γ-decay properties are in agreement with our microscopic, parameter free model predictions. For the first time, a second γ band predicted in ^{186}Hg has also been observed. This result shows that the coexistence picture so far established for $K = 0$ bands can be extended to other collective excitations.

To further expand present knowledge of the complex transitional region spanned by the neutron-deficient Hg isotopes, collective model calculations have also been performed for ^{184}Hg and ^{188}Hg. From a comparison between our theoretical model predictions and available experimental results, it is stressed that the coexistence picture at normal deformation is valid for the lighter Hg isotopes but ruled out for ^{190}Hg. This isotope is a γ-soft nucleus in which the excited $K = 0$ band is here interpreted as a quasi-β-band. Lifetime measurements are needed to further assess the validity of our model predictions.

ACKNOWLEDGMENTS

We would like to thank the staff of the ISOCELE facility for having provided us with constant intensity Tl beams during lengthy runs. We are indebted to the staff of the Orsay synchrocyclotron for their cooperation. We also thank the Service Electronique de l'Institut de Physique Nucléaire d'Orsay for technical support with the data acquisition system, and especially R. Breuil who took part in the experiments. We are grateful to Professor J. F. Sharpey-Schafer for careful reading of the manuscript.

[1] J. Bonn, G. Huber, H.-J. Kluge, L. Kugler, and E. W. Otten, Phys. Lett. **38B**, 308 (1972).
[2] P. Dabkiewicz, F. Buchinger, H. Fisher, H.-J. Kluge, H. Kremmling, T. Kühl, A. C. Müller, and H. A. Schuessler, Phys. Lett. **82B**, 199 (1979).
[3] G. Ulm, S. K. Bhattacherjee, P. Dabkiewicz, G. Huber, H.-J. Kluge, T. Kühl, H. Lochmann, E.-W. Otten, K. Wendt, S. A. Ahmad, W. Klempt, and R. Neugart, Z. Phys. A **325**, 247 (1986).
[4] M. Cailliau, J. Letessier, H. Flocard, and P. Quentin, Phys. Lett. **46B**, 11 (1973).
[5] U. Götz, H. C. Pauli, K. Alder, and K. Junker, Nucl. Phys. **A192**, 1 (1972).
[6] F. Dickmann and K. Dietrich, Z. Phys. A **263**, 211 (1973).
[7] K. Heyde, P. Van Isacker, M. Waroquier, J. L. Wood, and R. A. Meyer, Phys. Rep. **102**, 291 (1983); J. H. Hamilton, P. G. Hansen, and E. F. Zganjar, Rep. Prog. Phys. **48**, 631 (1985); J. L. Wood, K. Heyde, W. Nazarewicz, M. Huyse, and P. Van Duppen, Phys. Rep. **215**, 101 (1992), and references therein.
[8] D. Proetel, R. M. Diamond, P. Kienle, J. R. Leigh, K. H. Maier, and F. S. Stephens, Phys. Rev. Lett. **31**, 896 (1973).
[9] D. Proetel, R. M. Diamond, and F. S. Stephens, Phys. Lett. **48B**, 102 (1974).
[10] R. Béraud, M. Meyer, M. G. Desthuilliers, C. Bourgeois, P. Kilcher, and J. Letessier, Nucl. Phys. **A284**, 221 (1977).
[11] J. D. Cole *et al.*, Phys. Rev. C **16**, 2010 (1977).
[12] R. V. F. Janssens *et al.*, Phys. Lett. **131B**, 35 (1983).
[13] W. C. Ma, A. V. Ramayya, J. H. Hamilton, S. J. Robinson, J. D. Cole, E. F. Zganjar, E. H. Spejewski, R. Bengtsson, W. Nazarewicz, and J.-Y. Zhang, Phys. Lett. **167B**, 277 (1986).
[14] M. G. Porquet, G. Bastin, C. Bourgeois, A. Korichi, N. Perrin, H. Sergolle, and F. A. Beck, J. Phys. G **18**, L29 (1992), and references therein; W. C. Ma *et al.*, Phys. Rev. C **47**, R5 (1993).
[15] G. D. Dracoulis, A. E. Stuchbery, A. O. Macchiavelli, C. W. Beausang, J. Burde, M. A. Deleplanque, R. M. Diamond, and F. S. Stephens, Phys. Lett. B **208**, 365 (1988).
[16] W. C. Ma, A. V. Ramayya, J. H. Hamilton, S. J. Robinson, M. E. Barclay, K. Zhao, J. D. Cole, E. F. Zganjar, and E. H. Spejewski, Phys. Lett. **139B**, 276 (1984).
[17] N. Rud, D. Ward, H. R. Andrews, R. L. Graham, and J. S. Geiger, Phys. Rev. Lett. **31**, 1421 (1973); J. D. Cole *et al.*, *ibid.* **37**, 1185 (1976); W. C. Ma, A. V. Ramayya, J. H. Hamilton, S. J. Robinson, J. D. Cole, E. F. Zganjar, E. H. Spejewski, R. Bengtsson, W. Nazarewicz, and J. Y. Zhang, Phys. Lett. **167B**, 277 (1986).
[18] J. H. Hamilton *et al.*, Phys. Rev. Lett. **35**, 562 (1975); C. Bourgeois *et al.*, J. Phys. (Paris) **37**, 49 (1976); K. Hardt *et al.*, Z. Phys. A **312**, 251 (1983); J. D. Cole *et al.*, Phys. Rev. C **30**, 1267 (1984); F. Hannachi *et al.*, Nucl. Phys. **A481**, 135 (1988).
[19] R. Bengtsson, T. Bengtsson, J. Dudek, G. Leander, W. Nazarewicz, and J.-Y. Zhang, Phys. Lett. B **183**, 1 (1987).
[20] A. Faessler, U. Götz, B. Slavov, and T. Lederberger, Phys. Lett. **39B**, 579 (1972).
[21] S. Frauendorf and V. V. Pashkevich, Phys. Lett. **55B**, 365 (1975).

[22] R. Bengtsson, P. Möller, R. Nix, and J.-Y. Zhang, Phys. Scr. **29**, 402 (1984).
[23] J. Sauvage-Letessier, P. Quentin, and H. Flocard, Nucl. Phys. **A370**, 231 (1981).
[24] M. Girod and P. G. Reinhard, Phys. Lett. **117B**, 1 (1982).
[25] A. F. Barfield, B. R. Barrett, K. A. Sage, and P. D. Duval, Z. Phys. A **311**, 205 (1983); A. F. Barfield and B. R. Barrett, Phys. Lett. **149B**, 277 (1984).
[26] K. Heyde, J. Jolie, J. Moreau, J. Ryckebusch, M. Waroquier, P. Van Duppen, M. Huyse, and J. L. Wood, Nucl. Phys. **A466**, 189 (1987).
[27] J.-Y. Zhang and J. H. Hamilton, Phys. Lett. B **260**, 11 (1991).
[28] M. O. Kortelahti, E. F. Zganjar, J. L. Wood, C. R. Bingham, H. K. Carter, K. S. Toth, J. H. Hamilton, J. Kormicki, L. Chaturvedi, and W. B. Newbolt, Phys. Rev. C **43**, 484 (1991).
[29] J. P. Delaroche *et al.*, in International Workshop on Nuclear Shapes and Nuclear Structure at Low Excitation Energies, Cargèse, France, 1991, edited by M. Vergnes, J. Sauvage, P. H. Heenen, and H. T. Duong, NATO ASI Series No. B289 (Plenum, New York, 1992), Book of Abstracts, p. 16; J. Sauvage *et al.*, contribution to International Conference on the Future of Nuclear Spectroscopy, Crete, Greece (1993); J. Sauvage *et al.*, contribution to Eighth International Symposium on Capture Gamma-Ray Spectroscopy and Related Topics, Fribourg, Switzerland (1993).
[30] P. Ring and P. Schuck, *The Nuclear Many-Body Problem* (Springer, Berlin, 1980), p. 398.
[31] M. Girod and B. Grammaticos, Phys. Rev. C **27**, 2317 (1983).
[32] J. Dechargé and D. Gogny, Phys. Rev. C **21**, 1568 (1980); J. F. Berger, M. Girod, and D. Gogny, Nucl. Phys. **A428**, 23c (1984); **A502**, 85c (1989); Comput. Phys. Commun. **63**, 365 (1991).
[33] D. L. Hill and J. A. Wheeler, Phys. Rev. **89**, 1102 (1953); J. J. Griffin and J. A. Wheeler, *ibid.* **108**, 311 (1957).
[34] B. Giraud and B. Grammaticos, Nucl. Phys. **A233**, 373 (1974); **A255**, 141 (1975); M. Girod and B. Grammaticos, *ibid.* **A330**, 40 (1979), and references therein.
[35] K. Kumar and M. Baranger, Nucl. Phys. **A110**, 529 (1968); K. Kumar, B. Remaud, P. Auger, J. S. Vaagen, A. C. Rester, R. Foucher, and J. H. Hamilton, Phys. Rev. C **16**, 1235 (1977).
[36] K. Kumar, Nucl. Phys. **A231**, 189 (1974).
[37] D. Troltenier, J. A. Maruhn, W. Greiner, V. Velazquez Aguilar, P. O. Hess, and J. H. Hamilton, Z. Phys. A **338**, 261 (1991).
[38] M. Girod, J. P. Delaroche, D. Gogny, and J. F. Berger, Phys. Rev. Lett. **62**, 2452 (1989), and references therein; J. P. Delaroche, M. Girod, J. Libert, and I. Deloncle, Phys. Lett. B **232**, 145 (1989).
[39] F. Iachello, in *Interacting Bosons in Nuclear Physics*, edited by F. Iachello (Plenum, New York, 1979), p. 1.
[40] P. Paris *et al.*, Nucl. Instrum. Methods **186**, 91 (1981).
[41] B. Roussière, P. Kilcher, F. Le Blanc, J. Oms, J. Sauvage, and H. Dautet, Nucl. Phys. **A458**, 227 (1992).
[42] H. Hübel, A. P. Byrne, S. Ogaza, A. E. Stuchbery, G. D. Dracoulis, and M. Guttormsen, Nucl. Phys. **A453**, 316 (1986).
[43] C. R. Bingham *et al.*, Phys. Rev. C **14**, 1586 (1976).
[44] H. W. Taylor, B. Singh, F. S. Prato, and R. Mc Pherson, Nucl. Data Tables A **9**, 1 (1971).
[45] P. K. Joshi *et al.*, *Proceedings of the Sixth International Conference on Nuclei Far from Stability and Ninth International Conference on Atomic Masses and Fundamental Constants*, Bernkastel-Kues, Germany, 1992, edited by R. Neugart and A. Wöhr, IOP Conf. Proc. No. 132 (Institute of Physics and Physical Society, Bristol, 1993), p. 727; and (private communication).
[46] M. Girod, J. P. Delaroche, J. Libert, and I. Deloncle, Phys. Rev. C **45**, R1420 (1992); M. Girod, J. P. Delaroche, J. F. Berger, and J. Libert, Phys. Lett. B **325**, 1 (1994).